Inorganic Chemistry

Article

pubs.acs.org/IC

Inorganic Stressors of Ubiquitin

Giuseppe Arena,[†] Francesco Bellia,[‡] Giuseppina Frasca,[‡] Giulia Grasso,[‡] Valeria Lanza,[‡] Enrico Rizzarelli,[†,‡] Giovanni Tabbì,[‡] Valeria Zito,[‡] and Danilo Milardi*[,‡]

[†]Dipartimento di Scienze Chimiche, Università degli Studi di Catania, Viale Andrea Doria 6, 95125 Catania, Italy

[‡]Istituto di Biostrutture e Bioimmagini UOS—CT, Consiglio Nazionale delle Ricerche, Viale Andrea Doria 6, 95125 Catania, Italy

ABSTRACT: Many neurodegenerative proteinopathies are characterized by ubiquitin (Ub)-containing intraneuronal inclusion bodies. Recent reports have shown that Ub is able to bind Cu^{II} and Zn^{II}, the dyshomeostasis of which is a hallmark of neurodegeneration. Here we use complementary techniques like potentiometry, circular dichroism−visible, and electron spin resonance to unveil the Ub/metal species that form, at neutral pH, their binding constants and structural features. Next, we show that both Zn^{II} and Cu^{II} ions hinder the interactions between Ub and Ub-conjugating E2 enzymes and inhibit significantly both Lys48 and Lys63 self-polyubiquitination reactions in a cell-free medium. The effects of Zn^{II} and Cu^{II} on Lys63 and Lys48 polyUb chain synthesis are compatible with the hypothesis that metal binding to His68 modifies the Ile44 hydrophobic patch of Ub and makes the protein less available for polyUb. These findings contribute to further arguments for a close relationship between metal dyshomeostasis and abnormal protein degradative pathways in the upstream events, triggering neurodegeneration.

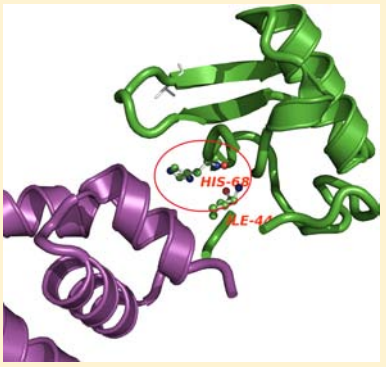

INTRODUCTION

Metal ions, such as copper (Cu) and zinc (Zn), are known to be normally involved in many neuronal pathways and are thus essential for brain function.[1] Their dysregulation, however, can initiate and progress a myriad of pathological pathways that may ultimately result in neurodegeneration.[2] Indeed, neurodegenerative disorders are known to share a common molecular mechanism involving protein misfolding and aggregation,[3,4] and accumulating evidence indicates that several adverse environmental factors, e.g., metal-ion dyshomeostasis, may accelerate these processes.[5−8] Notably, Cu^{II} and Zn^{II} ions can be found in abnormally large quantities in the inclusion bodies of patients with Alzheimer's (AD) and Parkinson's (PD) diseases, the two most common neurodegenerative disorders.[9,10]

One alleviatory measure employed by cells to protect the proteome from these adverse factors is to target misfolded proteins for clearance via the ubiquitin−proteasome system (UPS).[11,12]

Ubiquitin (Ub) is a protein composed of 76 amino acids, with a compact globular structure in which a mixed parallel/antiparallel β sheet packs against an α helix, generating a hydrophobic core.[13] Although Ub is best known as a prelude to proteasomal degradation, it also regulates a large array of biological processes, including protein translocation, signal transduction, gene transcription, apoptosis, and autophagy.[14] The correct functioning of the UPS requires the sequential intervention of three enzymes, E1, E2, and E3, having the ultimate goal of conjugating Ub to the target substrate.[15] The first step is always the formation of an isopeptide bond between the ε-amino group of a lysine of the target protein and the terminal −COOH of Ub. Noncovalent arrangements occurring between Ub and the E2-conjugating enzymes are significantly involved in the construction of polyubiquitin (polyUb) chains.[16] For example, the complex between Ub and E2-25K, an E2-conjugating enzyme that catalyzes the construction of Ub chains linked by Lys48, involves a hydrophobic interaction between Gly173, Phe174, and Leu198 of the E2 enzyme, on the one hand, and the Ile44 hydrophobic patch of Ub, on the other hand.[17] Such a hydrophobic binding has been observed for many other E2/Ub complexes and is thought to be essential for effective Ub chain growth.[18−24] The availability of seven lysine residues (Lys6, Lys11, Lys27, Lys29, Lys33, Lys48, and Lys63) enables Ub to form polyUb chains, each encoding different biological signals, the malfunctioning of which plays, unsurprisingly, an important role in various human pathological conditions, including neurodegenerative disorders.[25,26] The observation that protein aggregates within affected tissues often contain Ub further supports the correlation between UPS impairment and neurodegeneration.[27−30] More than a few biological investigations have demonstrated that exposure of the UPS to increasing amounts of metal ions affects its degradative activity, suggesting a close relationship between the age-dependent increase in the metal-ion concentration in the brain, UPS failure, and disease.[31,32]

Inspired by this evidence, we recently began in our laboratories a thorough investigation of Cu^{II} and Zn^{II} binding to Ub in solution. Cu^{II} ions have been found to bind Ub at a specific site involving the N-terminal N atom of Met1 and three O-donor ligands in a tetragonal geometry. The addition of Cu^{II} beyond a 1:1 ratio resulted in minor spectral changes also in the

Received: May 21, 2013
Published: July 26, 2013

   dx.doi.org/10.1021/ic401276x | *Inorg. Chem.* 2013, 52, 9567−9573

region around His68 (i.e., residues 66−68).[33] However, these experiments were performed only at pH 6.5. In a more recent paper focusing on Zn^{II}/Ub binding features, potentiometric titrations coupled with electrospray ionization mass spectrometry and NMR experiments evidenced that only two species, ZnUb and Zn_2Ub, are present in solution at neutral pH.[34] According to NMR evidence, Zn^{II} binds to a Ub region that is thought to be involved also in Cu^{II} binding and that would include Met1, Glu16, Val17, and Glu18 and a domain comprising Ile23, Glu24, Lys27, Ala28, Gln49, Glu51, Asp52, Arg54, and Thr55 residues. A second Zn^{II} binding site is centered on His68. These reports concerning metal−Ub interactions suggest that Cu^{II} and Zn^{II} binding to specific Ub regions might compromise its ability to self-conjugate in chains by hampering some key noncovalent protein−protein interactions.[33−35] However, the role of elevated levels of metal ions on Ub signaling is still an open problem.

In this work, we have first employed potentiometric titrations, circular dichroism (CD)−visible and electron spin resonance (ESR) experiments to determine the Cu^{II}- and Zn^{II}/Ub species that are predominant at neutral pH, as well as their stability constants and structural features. Next, sodium dodecyl sulfate−polyacrylamide gel electrophoresis (SDS-PAGE) experiments were carried out to demonstrate that Ub−E2 interactions may be hampered by Cu^{II} and Zn^{II} ions. Finally, Western blotting assays were performed to assess the impact of Cu^{II} and Zn^{II} ions on Lys48 and Lys63 self-polyubiquitination reactions in tube tests.

EXPERIMENTAL SECTION

Chemicals. Ub from bovine red cells was purchased from Biomol International and purified by extensive dialysis against pure water for 24 h at 48 °C, as reported elsewhere.[34] The protein concentration in pure water was measured by UV (ε_{280} = 1280 M^{-1} cm^{-1}).[36] $Cu(NO_3)_2{\cdot}5H_2O$ was purchased from Sigma-Aldrich (St. Louis, MO). Zn^{II} nitrate was prepared from Zn^{II} oxide by adding a slight excess of HNO_3. Stock solutions of HNO_3 and KOH were standardized by titration with primary standard tris(hydroxymethyl)-aminomethane and potassium hydrogenphthalate, respectively. Trehalose and dithiothreitol (DTT) were purchased from Fluka. Human recombinant Ub activating enzyme (UBE1), UbcH13/Uev heterodimer complex, and E2-25K were purchased from Boston Biochem. Standard solutions of diubiquitin (Ub_2), triubiquitin (Ub_3), and tetraubiquitin (Ub_4) chains and Lys63-linked Ub were purchased from ENZO Life Sciences. For SDS-PAGE, NuPAGE Novex Bis−Tris gels and 2-(*N*-morpholino)ethanesulfonic acid buffer were obtained from Invitrogen. For Western blotting, antimouse mono- and polyubiquitinylated conjugates, mAb (FK2) and goat antimouse IgG1-HRP antibody, were obtained from ENZO Life Sciences and Santa Cruz Biotechnology, respectively. All of the chemicals used, including ethyl-3-[3-(dimethylamino)propyl]carbodiimide hydrochloride (EDC), *N*-hydroxysuccinimide (NHS), and 3-(*N*-morpholino)-propanesulfonic acid (MOPS), were purchased from Sigma and were analytical grade, except silver nitrate, which was Sigma Ultra grade. All solutions were prepared with Milli-Q water.

ESR Experiments. A Bruker Elexsys E500 continuous-wave electron paramagnetic resonance (CW-EPR) spectrometer, driven by a PC running XEpr software and equipped with a Super-X microwave bridge operating at 9.3−9.5 GHz and a SHQE cavity, was used throughout this work. All EPR spectra of frozen solutions of Cu^{II} complexes were recorded at 150 K by means of a ER4131VT variable-temperature apparatus. In order to increase the spectral resolution, a small amount of methanol (not exceeding 10%) was added to the Cu^{II} complex aqueous solutions after adjustment of the pH to the desired value. Cu^{II}/Ub complexes (0.5 mM) were prepared by adding the proper amount of $^{63}Cu(NO_3)_2$ to Ub aqueous solutions containing a 100-fold excess of threalose (to avoid protein precipitation). EPR magnetic parameters were calculated from the second and third lines to get rid of second-order effects.[37] Instrumental settings of EPR spectra were as follows: number of scans, 8; microwave frequency, 9.370 GHz; modulation frequency, 100 kHz; modulation amplitude, 0.6 mT; time constant, 82 ms; microwave power, 40 mW; receiver gain, 54−60 dB.

pH-Metric Titrations. All pH-metric measurements were performed at 25 ± 0.2 °C using a homemade experimental apparatus that was described elsewhere.[38] The electrodic system (Metrohm combined LL micro-pH glass electrode) was calibrated on the pH scale by titrating HNO_3 with CO_2-free KOH (0.06 M). In order to prevent Ub aggregation, all solutions contained 0.1 M trehalose.[34] All titrations were run under an argon atmosphere to avoid any possible contamination by carbon dioxide and/or oxygen. Three independent Ub solutions were prepared, and precisely measured (Rainin EDP plus 2500) aliquots (ca. 1.800 mL) of each solution were titrated with KOH to determine the purity of the Ub batch and double-check the protonation constant values determined with different batches.[34] In order to determine the stability constants for Cu^{II}, appropriate aliquots of copper nitrate solutions were added to the above solutions of Ub. Copper nitrate solutions were standardized with ethylenediaminetetraacetic acid, as reported elsewhere.[39] The ligand concentration ranged from 7.6 × 10^{-4} to 7.9 × 10^{-4} M, while the metal-ion concentration ranged from 5.0 × 10^{-4} to 8.0 × 10^{-4} M. The resulting Cu^{II}/Ub solutions had metal-to-Ub ratios ranging from 1.04:1 to 1.04:1.57. A total of about 300 datapoints were collected over the pH 3.5−8.5 range for the five solutions prepared according to the procedure described above. Measured proton concentrations were used to determine the stoichiometry of each species and its overall stability constant (β) referring to the equilibrium

$$pCu + qUb + rH \rightleftarrows Cu_pUb_qH_r$$

and defined by the equation

$$\beta_{pqr} = \frac{[Cu_pUb_qH_r]}{[Cu]^p[Ub]^q[H]^r}$$

where β_{pqr}, $[Cu_pUb_qH_r]$, [Cu], [Ub], and [H] are the overall stability constants and the free concentrations of the complex, the metal ion, Ub, and the proton, respectively. Please note that *r* may have negative values.[40] Hyperquad was used to compute β values, the associated random errors (σ), and statistical parameters.[41] Additional details may be found elsewhere.[42]

CD. CD spectra were recorded with a Jasco J-810 spectropolarimeter by using a quartz cuvette with a 1 mm optical path and a 0.1 nm data pitch. All spectra, corresponding to an average of 10 scans, were base-line-corrected and then smoothed by applying adjacent averaging or an FFT filter. The Ub concentration in CD−UV Cu^{II} titration experiments (190−260 nm) was 7.8 μM. The Cu^{II}/Ub ratio ranged from 0.5 to 3.5. CD spectra of Ub in the visible region (260−750 nm) were obtained at a 1:1 metal-to-ligand ratio and in a (5−10) × 10^{-4} M protein concentration range. All spectra were recorded in pure water, and the pH was adjusted to 8.5 by adding NaOH.

Lys63 and Lys48 Auto-polyubiquitination Reactions in Tube Tests. Lys63-linked polyUb reactions were performed at pH 7.4 (*T* = 25 °C) in small volumes (40 μL) of a ligation buffer (50 mM MOPS, 5 mM $MgCl_2$, 0.5 mM DTT, and 2 mM ATP) containing Ub (5 μM), UBE1 (500 nM), and UbcH13/Uev (50 nM). Lys48 polyUb chain synthesis was carried out by mixing Ub (10 μM), UBE1 (100 nM), and E2-25K (1 μM) in the same experimental conditions as those used for Lys63 polyUb reactions. In order to prevent oxidation, the antioxidant agent DTT (0.5 mM) was added to the reaction buffer. Visible spectroscopy using the Cu^{I}-dependent absorption changes of bathocuproin at 483 nm[43] demonstrated that Cu^{II} is not reduced to Cu^{I} in the presence of DTT. All reactions were carried out at different metal-to-Ub molar ratios and constant Ub concentration. The reactions were quenched after 4 h of incubation, as described above, and size-fractioned by SDS-PAGE, as reported elsewhere.[44] They were then electrotransferred onto a nitrocellulose membrane (GE Health-

dx.doi.org/10.1021/ic401276x | Inorg. Chem. 2013, 52, 9567−9573

Care, Lifescience). Nonspecific antibody binding was blocked by incubation with 1% bovine serum albumin in phosphate buffered saline (PBS) for 1 h at room temperature. Blots were then probed with antimouse mono- and polyubiquitinylated conjugates mAb [clone FK2] (1:5000), overnight at 4 °C. After repeated washing with PBS and 0.1% Tween, membranes were incubated with goat antimouse IgG1-HRP antibody (1:10000). Specific bands were visualized by Supersignal West Pico Chemiluminescent Substrate (Thermo Scientific). All blots were routinely compared with a standard mix containing Cu^{II} and Zn^{II} (55 μM), free Ub, and Ub_2, Ub_3, and Ub_4 chains to ensure the full efficiency of antibodies in Cu^{II}- or Zn^{II}-loaded buffers.

Gel Electrophoresis. Ub (20 μM) was incubated on ice in 20 μL of a 50 mM MOPS buffer (pH 7.4), $MgCl_2$ (5 mM), and the E2-conjugating enzyme (i.e., E2-25K or, alternatively, human recombinant MMS2 from Boston Biochemicals) in the presence or in the absence of Cu^{II} (200 μM) or Zn^{II} (100 μM). After 3 h, the chemical cross-linkers EDC and NHS were added up to a final concentration 0.3 mM. Incubation was continued at 0 °C overnight. Solutions were then kept for 1 h at 20 °C. Next, chemical cross-linking was quenched by dilution with the loading buffer containing 8% (w/v) SDS, 24% (v/v) glycerol, 0.015% Coomassie Blue G, and aliquots analyzed by SDS-PAGE. The gels were stained by the conventional Ag-staining procedure.[45]

RESULTS AND DISCUSSION

Characterization of Cu^{II}/Ub Species in Solution: Potentiometric Titrations. A previous study at pH 6.5 has shown that Cu^{II} binds to the NH_2-terminus of Ub.[33] Here we investigate a wider pH range to prove (or disprove) whether His68 is a site of anchoring for Cu^{II} at neutral pH. To this aim, we resorted to potentiometric titrations to unveil all Cu^{II}/Ub binding equilibria in solution. Ub protonation constants have been reported in a previous work;[34] the protonation constant values have been double-checked by using the protein batches employed for determination of the Cu^{II}/Ub stability constants and match the published values. Figure 1 shows typical pH-metric titration curves collected both in the absence and in the presence of Cu^{II} ions.

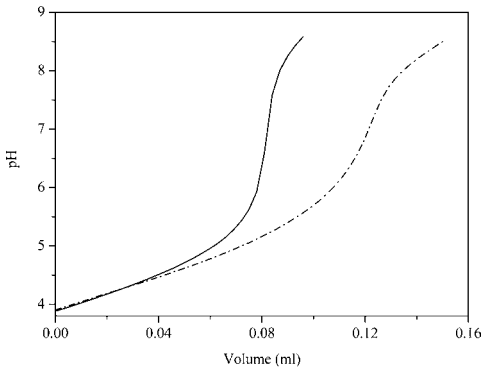

Figure 1. pH-metric titrations in the absence (continuous line) and in the presence (broken line) of Cu^{II} ions ($C_{Cu^{II}} = 5 \times 10^{-4}$ M; $C_{Ub} = 7 \times 10^{-4}$ M).

The large proton displacement caused by the presence of Cu^{II} ions shows that they form fairly stable complexes with Ub as the pH increases. The superimposition of the curves up to pH 4 indicates that Ub starts to interact appreciably with Cu^{II} only above this pH value and that complexation becomes significant over the physiological pH range.

The pH-metric titration curves collected in the presence of Cu^{II} under different metal-to-ligand ratios were satisfactorily fitted (Figure 2) by the set of constants listed in Table 1.

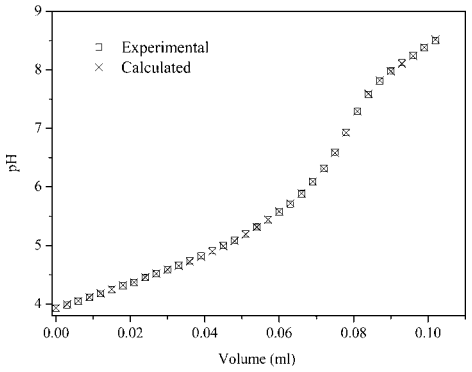

Figure 2. pH-metric titration of a solution containing Cu^{II} ions and Ub ($C_{Cu} = C_{Ub} = 7 \times 10^{-4}$ M).

Table 1. log β for Complexes of Cu^{II} with Ub at 25 °C and 0.1 M Trehalose

equilibrium	β_{pqr} [a]	log β [b]
Cu + Ub ⇄ CuUb	β_{110}	6.16(3)
Cu + Ub ⇄ $CuUbH_{-1}$ + H	β_{11-1}	−1.54(6)
2Cu + Ub ⇄ Cu_2UbH_{-4} + 4H	β_{21-4}	−20.5(1)
Cu + Ub ⇄ $CuUbH_{-4}$ + 4H	β_{11-4}	−27.27(8)

[a] For symbolism, see the Experimental Section. [b] Standard deviation in parentheses. Charges are omitted for simplicity.

Obviously, this set of constants was not the only one tested to fit the experimental data. Although several species were tested in different combinations to fit the experimental data, the best fit was invariably obtained with the set shown in Table 1. Two species ([CuUb] and $[CuUbH_{-1}]$ form over the physiological pH range; the stability constant value of the major species ([CuUb]; Figure 3) is consistent with the

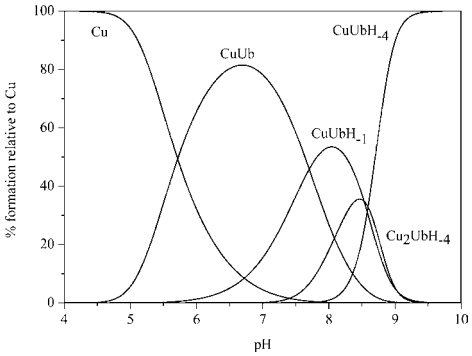

Figure 3. Species distribution for the Cu/Ub system ($C_{Cu} = 9 \times 10^{-4}$ M; $C_{Ub} = 1.3 \times 10^{-3}$ M).

coordination environment deduced previously from NMR experiments.[33] This species loses a proton from an amide N atom of the peptide backbone as the pH increases, leading to the formation of $[CuUbH_{-1}]$. As the pH is further increased, two new species form (viz., $[Cu_2UbH_{-4}]$ and $[CuUbH_{-4}]$); notably, these species form in significant amounts well above pH 7.5 and, consequently, are of limited relevance in physiological conditions.

dx.doi.org/10.1021/ic401276x | Inorg. Chem. 2013, 52, 9567−9573

Cu^{II} Complexes of Ub: His68 Is a Favored Anchoring Site at Neutral pH. Far-UV−CD analysis of Ub in the absence of metal ions evidences both a positive band (λ = 195 nm) and two negative bands (λ = 208 and 220 nm) that are characteristic of an α-helical conformation (data not shown).[33] The addition of Cu^{II} ions to Ub solutions at physiological pH causes no major conformational changes, regardless of the metal-to-ligand ratio. Even in the presence of excess protein, i.e., at a 1:2 Cu^{II}/Ub ratio, the protein maintains its prevalently α-helical conformation within the pH 5−10 range. A low-intensity band (λ = 280 nm) is detected in the pH range of formation of [CuUb]. Such a band and the absence of any detectable d−d band are diagnostic of the binding of the amine N atom to Cu^{II}.[46] It is worth noting that a band ($\lambda \sim$ 260 nm) typical of a $N_{im} \rightarrow Cu^{II}$ charge-transfer transition appears around neutrality and becomes increasingly more intense as the pH increases (Figure 4).

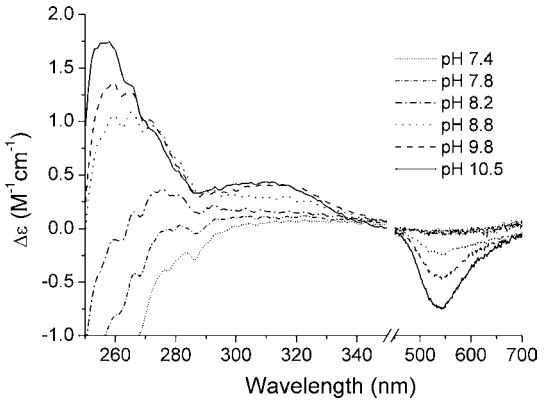

Figure 4. CD spectra of Cu^{II}/Ub mixtures at a 1:1 metal-to-ligand ratio in pure water at different pH values.

A new band (λ = 310 nm), paralleled by a band at λ = 550 nm, is detected at higher pH values; both of these bands are characteristic of a Cu^{II} complex involving a $N^- \rightarrow Cu^{II}$ charge transfer, while the presence of a d−d transition band indicates the formation of a chelate ring involving both the imidazole and peptide amide N atoms. ESR measurements at 150 K of solutions containing equimolar concentrations of Cu^{II} and Ub at different pH values support the picture derived from the CD experiments (Figure 5). The Hamiltonian parameters extracted from these spectra are listed in Table 2. The spectrum at the lowest pH value evidences a single species having $g_{\|}$ and $A_{\|}$ values that are in line with previous data[24] and can be attributed to a 1N3O coordination environment (Figure 5a). The above parameters are indicative of coordination of an amine N atom and a carboxylic O atom, while the remaining two O atoms of the 1N3O coordination environment are likely provided by two water molecules. The N atom comes from the Met1 N-terminal amino moiety, that is, the most basic Cu^{II} anchoring site of the protein, as evidenced by paramagnetic NMR studies,[33] while potential alternative O donor ligands are Met1 and Val17 (carbonyl groups) and Glu16 and Glu18 (carboxylate groups).

A preliminary investigation performed by using the AM1 method[47] shows that these two coordination environments have comparable energies and hence are equally possible or may interconvert from one to the other, suggesting the formation of isomeric species. The species characterized by such a chromophore corresponds to the [CuUb] species

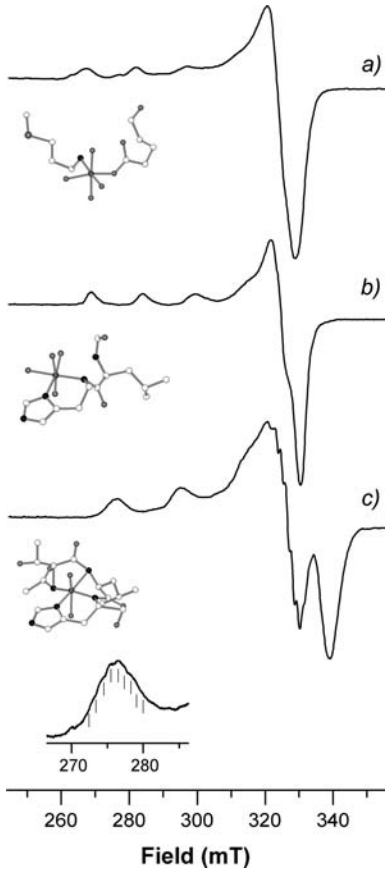

Figure 5. Frozen-solution EPR spectra of a Cu^{II}/Ub system (C_{Ub} = C_{Cu} = 0.8 mM) at pH 6.5 (a), 8.0 (b), and 10 (c). The inset of part c shows the superhyperfine pattern of the first line in the spectrum. Sketches of the proposed coordination environments for each species are shown.

Table 2. Hamiltonian Parameters at Different pH Values[a]

pH	$g_{\|}$	$A_{\|} \times 10^4$ (cm^{-1})
6.5	2.310(5)	158(3)
8.0	2.288(3)	167(3)
10	2.195(3)	197(3)

[a]Parameters extracted from the spectra shown in Figure 7; C_{Ub} = C_{Cu} = 0.8 mM. Estimated errors on the last decimal figure in parentheses.

detected by potentiometric measurements (Figure 3). At the highest pH value (Figure 5c), the ESR spectrum shows the formation of a species with Hamiltonian parameters indicative of the coordination of four in-plane N atoms;[48−50] such a coordination environment is supported by the nine-line superhyperfine structure (inset of Figure 5c). The ESR study matches the potentiometric results; the above species corresponds to the [$CuUbH_{-4}$] species that according to the potentiometric investigation prevails above pH 8 (Figure 3). At pH values between 6.5 and 10, the ESR spectrum is characterized by $g_{\|}$ and $A_{\|}$ values equal to 2.288 and 167 × 10^{-4} cm^{-1} (Figure 5b and Table 2). The pH increase parallels the decrease of $g_{\|}$ values and the increase of $A_{\|}$ values, indicating that the anchoring of Cu^{II} to the histidine imidazole N atom favors deprotonation of the amide N atoms.[51] The ESR study has not provided evidence for formation of the binuclear species detected potentiometrically. This is probably due to either a prevalence of the [$CuUbH_{-1}$] species over

dx.doi.org/10.1021/ic401276x | Inorg. Chem. 2013, 52, 9567−9573

$[Cu_2UbH_{-4}]$ at 150 K or dipolar interactions between the Cu^{II} centers, which, in turn, lead to a broadening of the spectrum. The potentiometric and ESR results lead one to conclude that Ub possesses at least two sites for Cu^{II} coordination that can be differently populated depending on the pH of the medium; it is wroth noting that the Cu^{II} species with Cu anchored to His68 is significantly populated at neutral pH (around 30%).

Cu^{II} and Zn^{II} Ions Competing for the His68 Residue of Ub. Similar to Cu^{II}, Zn^{II} also binds to Ub,[34] forming two main species, $[Zn_2Ub]$ and [ZnUb], in the physiological pH range. As the pH increases, four more protons are lost and the resulting species, $[Zn_2UbH_{-4}]$, predominates. However, because this metal ion is diamagnetic, EPR cannot be employed to evaluate Zn^{II} coordination features. Moreover, NMR experiments can be performed only at pH values lower than 7 to avoid aggregation. Thus, a direct involvement of His68 imidazole in Zn^{II} binding at neutral pH may be inferred only by extrapolating the NMR results obtained previously.[34] In order to further address this issue, we monitored $Cu^{II}-Zn^{II}$ competition by CD (Figure 6). To this end, Ub was incubated

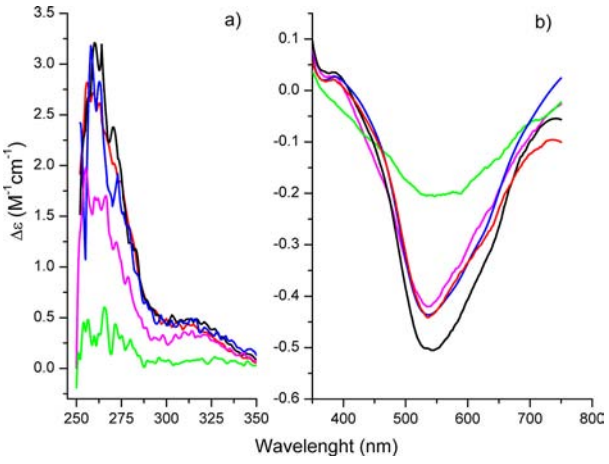

Figure 6. CD spectra of Cu^{II}/Zn^{II}/Ub mixtures ($C_{Ub} = 4.8 \times 10^{-4}$ M; pH 8.5) recorded in the ranges 250−350 nm (panel a) and 350−800 nm (panel b) at different Cu:Zn molar ratios: $Cu^{II}:Zn^{II}$:Ub = 3:0:1 (black); $Cu^{II}:Zn^{II}$:Ub = 3:0.5:1 (red), $Cu^{II}:Zn^{II}$:Ub = 3:1:1 (blue); $Cu^{II}:Zn^{II}$:Ub = 3:2:1 (purple); $Cu^{II}:Zn^{II}$:Ub = 3:3:1 (green).

with a 3-fold molar excess of Cu^{II}; Zn^{II} was then added to the Cu/Ub solution up to a 3:3:1 molar ratio (Cu:Zn:Ub). The far-UV and d−d CD bands, characteristic of the Cu^{II} complexes with Ub, decrease upon increasing Zn^{II} concentration, showing that equimolar Zn^{II} concentrations displace Cu^{II} from Ub. The CD bands become fairly visible slightly above the physiological pH. The results illustrated in Figure 6 may be interpreted by the species distribution diagrams (Figure 7) obtained using the set of binding constants obtained in both the present work and previous experiments.[34] The distribution diagrams show that Cu^{II}/Ub species progressively decrease as the Zn^{II} concentration increases and become insignificant at 3:3:1 ratios (Figure 7c). This nicely matches the CD experiments, which show that Cu^{II} bands are no longer detected when using equimolar Cu:Zn ratios (Figure 6b). Therefore, Zn^{II} tends to compete with Cu^{II} by shifting Cu complexation toward sites that minimize its interaction with histidines, as observed elsewhere.[52,53]

Cu^{II} and Zn^{II} Ions Hindering Interactions between Ub and E2. Next, mixtures of Ub and E2-25K, an E2 enzyme that

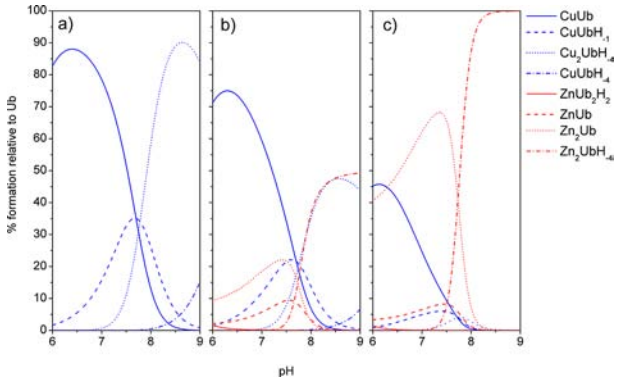

Figure 7. Species distribution for the Cu^{II}/Zn^{II}/Ub system calculated in the same experimental conditions as those used for CD experiments at different Cu^{II}/Zn^{II} molar ratios: Cu:Zn:Ub = 3:0:1 (panel a); Cu:Zn:Ub = 3:1:1 (panel b); Cu:Zn:Ub = 3:3:1 (panel c).

catalyzes the growth of Lys48-linked polyUb chains, were incubated with Cu^{II} or Zn^{II} metal ions and analyzed by SDS-PAGE. SDS-PAGE of metal-free control mixtures of Ub/E2-25K (~33 kDa) shows a band corresponding to the apparent molecular weight of the Ub/E2 assembly (Figure 8, upper right panel, lane 5), which clearly indicates an interaction between the two proteins. By contrast, SDS-PAGE of Ub/E2-25K mixtures incubated in the presence of excess Cu^{II} or Zn^{II} lacks this band (Figure 8, upper right panel, lane 4, and upper left panel, lane 3). Analogously, SDS-PAGE of MMS2, an enzyme that catalyzes the formation of Lys63-linked polyUb chains, incubated with Ub shows a band at ~25 kDa, corresponding to the apparent molecular weight of the Ub/MMS2 assembly (Figure 8, lower right panel, lane 6); this band disappears for Ub/E2 mixtures incubated in the presence of excess Cu^{II} or Zn^{II} ions (Figure 8, lower right panel, lane 5, and lower left panel, lane 3). These data suggest that both Cu^{II} and Zn^{II} ions hinder Ub−E2 interactions. Given the proximity of His68 and Ile44 in Ub, it may be conceived that metal binding to Ub may affect the E2/Ub assembly. These data cannot exclude that metal ions can also bind to E2. However, because MMS2 (pdb code: 1ZGU) does not have His residues, it is implausible that it may bind Cu^{II} or Zn^{II} with high affinity at physiological pH values. On the other hand, E2-25K (pdb code: 3K9P) has two His residues (namely, His81 and His150) that may potentially bind metal ions. It is unlikely that such an interaction could influence Ub/E2 association because (i) Western blot tests show that E2-25K gives results analogous to those found for MMS2 and (ii) the crystal structure of the E2-25K/Ub complex shows that the two His residues of E2-25K are far from the actual E2-25K/Ub interaction region. All of these considerations suggest that the binding of the metal ion to the His residue of Ub hinders Ub−E2 interactions.

Cu^{II} and Zn^{II} Ions Inhibiting Lys63 and Lys48 Self-polyubiquitination Reactions. Next, we investigated the effect of Cu^{II} and Zn^{II} ions on Lys63-linked polyUb chain synthesis. Lys63-linked polyUb chain synthesis was challenged by increasing Cu^{II} concentrations from 15 to 55 μM, i.e., from 3:1 to 11:1 metal-to-Ub molar ratios, respectively (Figure 9, left panel). PolyUb chain synthesis is inhibited in a Cu^{II}-concentration-dependent manner, as evidenced by the decreased density of the blots corresponding to Ub_2, Ub_3, Ub_4, and Ub_5. The polyUb reaction is significantly inhibited at a Cu^{II} concentration of ~45 μM (i.e., a 9:1 metal-to-ligand molar ratio), while it is fully quenched at 55 μM. The same effects,

dx.doi.org/10.1021/ic401276x | Inorg. Chem. 2013, 52, 9567−9573

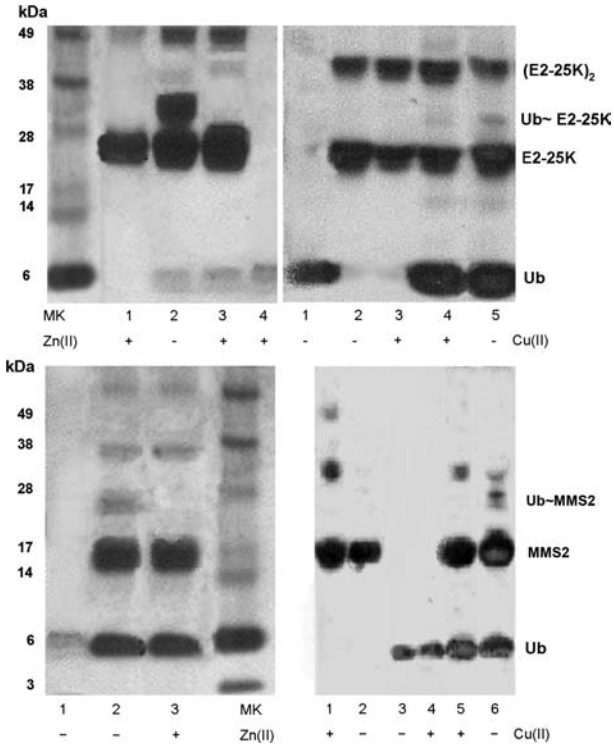

Figure 8. Effect of Cu^{II} (right) and Zn^{II} (left) ions on the noncovalent interactions occurring between Ub and E2 enzymes, E2-25K (UbcH1) (upper panel) and MMS2 (Uev2) (lower panel). Upper panel, left: lane 1, E2-25K (8 μM); lane 2, Ub (20 μM), E2-25K (8 μM); lane 3, Ub (20 μM), E2-25K (8 μM), Zn^{II} (100 μM); lane 4, Ub (20 μM). Upper panel, right: lane 1, Ub (20 μM); lane 2, E2-25K (8 μM); lane 3, E2-25K (8 μM), Cu^{II} (200 μM); lane 4, Ub (20 μM), E2-25K (8 μM), Cu^{II} (200 μM); lane 5, Ub (20 μM), E2-25K (8 μM). Lower panel, left: lane 1, Ub (20 μM); lane 2, Ub (20 μM), MMS2 (8 μM); lane 3, Ub (20 μM), MMS2 (8 μM), Zn^{II} (100 μM). Lower panel, right: lane 1, MMS2 (8 μM), Cu^{II} (200 μM); lane 2, MMS2 (8 μM); lane 3, Ub (20 μM); lane 4, Ub (20 μM), Cu^{II} (200 μM); lane 5, Ub (20 μM), MMS2 (8 μM), Cu^{II} (200 μM); lane 6, Ub (20 μM), MMS2 (8 μM).

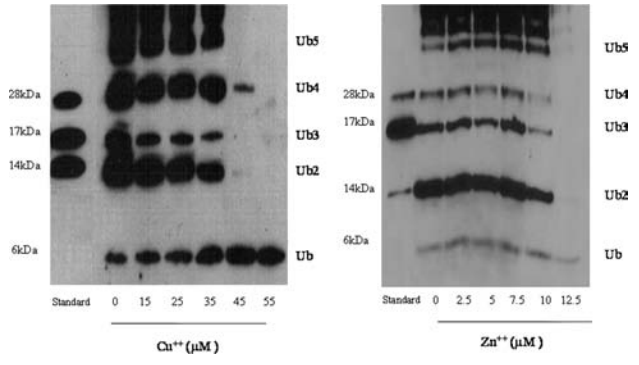

Figure 9. Lys63-linked polyUb chain synthesis activity of the UbcH13/Uev1A heterodimer complex in the presence of Cu^{II} (left) or Zn^{II} (right) ions.

although at a lower metal concentration, are evidenced when Zn^{II} ions were added to the reaction mixture (see Figure 9, right panel).

In analogy to Lys63-linked polyUb reactions, we also performed Lys48-linked polyUb reactions in the presence of increasing amounts of Cu^{II} and Zn^{II} ions (Figure 10). The figure evidences that upon the addition of Cu^{II} (50 μM) the

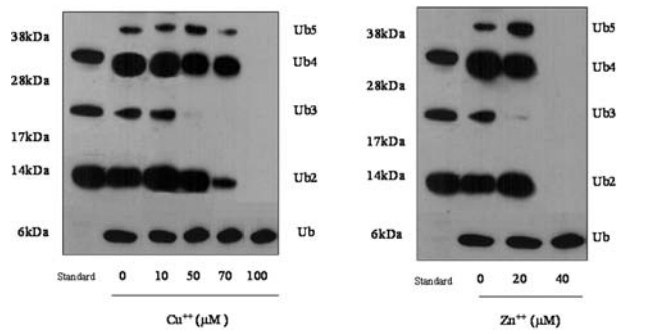

Figure 10. Lys48 polyUb chain synthesis activity of the E2-25K enzyme in the presence of Cu^{II} (left) and Zn^{II} (right) ions. Assays and Western blotting were performed as described in the Experimental Section.

polyUb reaction is significantly inhibited. The effect is even more pronounced in the presence of larger concentrations (70 μM) and suggests a Cu^{II}-dependent inhibition mechanism similar to that observed for Lys63 polyUb reactions. In polyUb reactions occurring at Lys48, these phenomena are evidenced at a higher Cu^{II} concentration than in those taking place at Lys63. Notably, a concentration of Zn^{II} of 40 μM is sufficient to inhibit the reaction.

CONCLUSIONS

Post-translational modifications of proteins with Ub are thought to control many cellular processes including clearance of amyloid proteins. Thus, it is not surprising that Ub is commonly found within insoluble aggregates characteristic of neurodegenerative disorders where its presence reflects abnormal tagging of misfolded proteins. Adverse environmental factors may affect the Ub physicochemical features; among them, an increase of Cu^{II} levels has been recently proposed to destabilize Ub, leading Cu^{II}/Ub complexes to the formation of SDS-resistant oligomers.[33,35] Zn^{II} ions were also shown to bind Ub, leading to oligomeric assemblies.[34]

Here we provide evidence showing that at neutral pH Cu^{II} may bind to His68 with a coordination environment formed by an imidazolic N atom, its deprotonated amide, and two water molecules. Zn^{II} competes effectively with Cu^{II} for the same Ub region, and both metal ions hinder the interactions of Ub with E2-conjugating enzymes E2-25K and MMS2. This may be ascribed to the binding of Cu^{II} and Zn^{II} to His68, which is located in the proximity of the Ile44 hydrophobic patch of Ub. Both metals, at concentrations ranging from 45 to 70 μM for Cu^{II} and from 12 to 40 μM for Zn^{II}, are able to block polyUb reactions proceeding through linkage to Lys63 and Lys48, respectively.

The results of this study indicate that, at neutral pH, Cu^{II} and Zn^{II} binding to Ub might block Ub conjugation machinery occurring at either Lys63 or Lys48 with possible repercussions on Ub signaling.

AUTHOR INFORMATION

Corresponding Author

*E-mail: dmilardi@unict.it. Fax: (+)39-95-337678.

Notes

The authors declare no competing financial interest.

■ ACKNOWLEDGMENTS

This work was financially supported by MIUR (PRIN 2010M2JARJ, PRIN 2009WCNS5C_002, PRIN 2008F5A3AF_005, and RBNE08HWLZ-MERIT) and the University of Catania (PRA).

■ REFERENCES

(1) Kepp, K. P. *Chem. Rev.* **2012**, *112*, 5193−5239.
(2) Nunomura, A.; Perry, G.; Aliev, G.; Hirai, K.; Takeda, A.; Balraj, E. K.; Jones, P. K.; Ghanbari, H.; Wataya, T.; Shimohama, S.; Chiba, S.; Atwood, C. S.; Petersen, R. B.; Smith, M. A. *J. Neuropathol. Exp. Neurol.* **2001**, *60*, 759−767.
(3) Soto, C. *Nat. Rev. Neurosci.* **2003**, *4*, 49−60.
(4) Chiti, F.; Dobson, C. M. *Annu. Rev. Biochem.* **2006**, *75*, 333−366.
(5) Brown, D. R.; Qin, K.; Herms, J. W.; Madlung, A.; Manson, J.; Strome, R.; Fraser, P. E.; Kruck, T. A.; von Bohlen, A.; Schulz-Schaeffer, W.; Giese, A.; Westaway, D.; Kretzschmar, H. *Nature* **1997**, *390*, 684−687.
(6) Atwood, C. S.; Moir, R. D.; Huang, X.; Scarpa, R. C.; Bacarra, N. M.; Romano, D. M.; Hartshorn, M. A.; Tanzi, R. E.; Bush, A. I. *J. Biol. Chem.* **1998**, *273*, 12817−12826.
(7) Paik, S. R.; Shin, H. J.; Lee, J. H.; Chang, C. S.; Kim, J. *Biochem. J.* **1999**, *340*, 821−828.
(8) Morgan, C. J.; Gelfand, M.; Atreya, C.; Miranker, A. D. *J. Mol. Biol.* **2001**, *309*, 339−345.
(9) Bush, A. I. *Trends Neurosci.* **2003**, *26*, 207−214.
(10) Barnham, K. J.; Bush, A. I. *Curr. Opin. Chem. Biol.* **2008**, *12*, 222−228.
(11) Powers, E. T.; Morimoto, R. I.; Dillin, A.; Kelly, J. W.; Balch, W. E. *Annu. Rev. Biochem.* **2009**, *78*, 959−991.
(12) Pickart, C. M. *Annu. Rev. Biochem.* **2001**, *70*, 503−533.
(13) Vijay-Kumar, S.; Bugg, C. E.; Cook, W. J. *J. Mol. Biol.* **1987**, *194*, 531−544.
(14) Mukhopadhyay, D.; Riezman, H. *Science* **2007**, *315*, 201−205.
(15) Hershko, A.; Heller, H.; Elias, S.; Ciechanover, A. *J. Biol. Chem.* **1983**, *258*, 8206−8214.
(16) Sjoerd, J.; van Wijk, L.; Marc Timmers, H. T. *FASEB J.* **2010**, *24*, 981−993.
(17) Wilson, R. C.; Edmondson, S. P.; Flatt, J. W.; Helms, K.; Twigg, P. D. *Biochem. Biophys. Res. Commun.* **2011**, *405*, 662−666.
(18) Swanson, K. A.; Hicke, L.; Radhakrishnan, I. *J. Mol. Biol.* **2006**, *358*, 713−724.
(19) Mueller, T. D.; Feigon, J. *J. Mol. Biol.* **2002**, *319*, 1243−1255.
(20) Mueller, T. D.; Kamionka, M.; Feigon, J. *J. Biol. Chem.* **2004**, *279*, 11926−11936.
(21) Hofmann, R. M.; Pickart, C. M. *Cell* **1999**, *96*, 645−653.
(22) VanDemark, A. P.; Hofmann, R. M.; Tsui, C.; Pickart, C. M.; Wolberger, C. *Cell* **2001**, *105*, 711−720.
(23) McKenna, S.; Spyracopoulos, L.; Moraes, T.; Pastushok, L.; Ptak, C.; Xiao, W.; Ellison, M. J. *J. Biol. Chem.* **2001**, *276*, 40120−40126.
(24) McKenna, S.; Moraes, T.; Pastushok, L.; Ptak, C.; Xiao, W.; Spyracopoulos, L.; Ellison, M. J. *J. Biol. Chem.* **2003**, *278*, 13151−13158.
(25) Ciechanover, A.; Schwartz, A. L. *Proc. Natl. Acad. Sci. U.S.A.* **1998**, *95*, 2727−2730.
(26) Lehman, N. L. *Acta Neuropathol.* **2009**, *118*, 329−347.
(27) Lowe, J.; Blanchard, A.; Morrell, K.; Lennox, G.; Reynolds, L.; Billett, M.; Landon, M.; Mayer, R. J. *J. Pathol.* **1988**, *155*, 9−15.
(28) Ciechanover, A.; Brundin, P. *Neuron* **2003**, *40*, 427−446.
(29) Ross, C. A.; Pickart, C. M. *Trends Cell. Biol.* **2004**, *14*, 703−711.
(30) Lowe, J.; Hand, N.; Mayer, R. J. *Methods Enzymol.* **2005**, *399*, 86−119.
(31) Amici, M.; Forti, K.; Nobili, C.; Lupidi, G.; Angeletti, M.; Fioretti, E.; Eleuteri, A. M. *J. Biol. Inorg. Chem.* **2002**, *7*, 750−756.
(32) Santoro, A. M.; Lo Giudice, M. C.; D'Urso, A.; Lauceri, R.; Purrello, R.; Milardi, D. *J. Am. Chem. Soc.* **2012**, *134*, 10451−10457.
(33) Milardi, D.; Arnesano, F.; Grasso, G.; Magrì, A.; Tabbì, G.; Scintilla, S.; Natile, G.; Rizzarelli, E. *Angew. Chem., Int. Ed.* **2007**, *46*, 7993−7995.
(34) Arena, G.; Fattorusso, R.; Grasso, G.; Grasso, G. I.; Isernia, C.; Malgieri, G.; Milardi, D.; Rizzarelli, E. *Chem.—Eur. J.* **2011**, *17*, 11596−11603.
(35) Arnesano, F.; Scintilla, S.; Calò, V.; Bonfrate, E.; Ingrosso, C.; Losacco, M.; Pellegrino, T.; Rizzarelli, E.; Natile, G. *PLoS One* **2009**, *4*, e7052.
(36) Wintrode, P. L.; Makhatadze, G. I.; Privalov, P. L. *Proteins Struct. Funct. Bioinf.* **1994**, *18*, 246−253.
(37) Lund, A.; Vanngard, T. *J. Chem. Phys.* **1969**, *50*, 2979−2980.
(38) Grasso, G. I.; Arena, G.; Bellia, F.; Maccarrone, G.; Parrinello, M.; Pietropaolo, A.; Vecchio, G.; Rizzarelli, E. *Chem.—Eur. J.* **2011**, *17*, 9448−9455.
(39) Flashka, H. A. *EDTA Titrations*; Pergamon Press: London, 1959.
(40) Arena, G.; Pappalardo, G.; Sovago, I.; Rizzarelli, E. *Coord. Chem. Rev.* **2012**, *256*, 3−12.
(41) Gans, P.; Sabatini, A.; Vacca, A. *J. Chem. Soc., Dalton Trans.* **1985**, 1195−1200.
(42) Arena, G.; Calì, R.; Rizzarelli, E.; Sammartano, S. *Transition Met. Chem.* **1978**, *3*, 147−152.
(43) Crumbliss, A. L.; Poulos, A. T. *Inorg. Chem.* **1975**, *14*, 1529−1534.
(44) Piotrowski, J.; Beal, R.; Hoffman, L.; Wilkinson, K. D.; Cohen, R. E.; Pickart, C. M. *J. Biol. Chem.* **1997**, *272*, 23712−23721.
(45) Chevallet, M.; Luche, S.; Rabilloud, T. *Nat. Protoc.* **2006**, *1*, 1852−1858.
(46) Travaglia, A.; Arena, G.; Fattorusso, R.; Isernia, C.; La Mendola, D.; Malgieri, G.; Nicoletti, V. G.; Rizzarelli, E. *Chem.—Eur. J.* **2011**, *17*, 3726−3738.
(47) Dewar, M. J. S.; Zoebisch, E. G.; Healy, E. F.; Stewart, J. J. P. *J. Am. Chem. Soc.* **1985**, *107*, 3902−3909.
(48) Bonomo, R. P.; Cucinotta, V.; D'Alessandro, F.; Impellizzeri, G.; Maccarrone, G.; Vecchio, G.; Rizzarelli, E. *Inorg. Chem.* **1991**, *30*, 2709−2713.
(49) Bonomo, R. P.; Conte, E.; Marchelli, R.; Santoro, A. M.; Tabbì, G. *J. Inorg. Biochem.* **1994**, *53*, 127−138.
(50) Bonomo, R. P.; De Flora, A.; Rizzarelli, E.; Santoro, A. M.; Tabbì, G.; Tonetti, M. *J. Inorg. Biochem.* **1995**, *59*, 773−784.
(51) La Mendola, D.; Bonomo, R. P.; Impellizzeri, G.; Maccarrone, G.; Pappalardo, G.; Pietropaolo, A.; Rizzarelli, E.; Zito, V. *J. Biol. Inorg. Chem.* **2005**, *10*, 463−475.
(52) Damante, C. A.; Ösz, K.; Nagy, Z.; Grasso, G.; Pappalardo, G.; Rizzarelli, E.; Sóvágó, I. *Inorg. Chem.* **2010**, *50*, 5342−5345.
(53) Walter, E. D.; Stevens, D. J.; Visconte, M. P.; Millhauser, G. L. *J. Am. Chem. Soc.* **2007**, *129*, 15440−15441.